Time-Domain Optimal Experimental Design in Human Seated Postural Control Testing

M. Cody Priess   Jongeun Choi   Clark Radcliffe

John M. Popovich Jr.   Jacek Cholewicki   N. Peter Reeves

Michigan State University

Technical Report

October 28, 2014

Abstract

We are developing a series of systems science-based clinical tools that will assist in modeling, diagnosing, and quantifying postural control deficits in human subjects. In line with this goal, we have designed and constructed a seated balance device and associated experimental task for identification of the human seated postural control system. In this work, we present a Quadratic Programming (QP) technique for optimizing a time-domain experimental input signal for this device. The goal of this optimization is to maximize the information present in the experiment, and therefore its ability to produce accurate estimates of several desired seated postural control parameters. To achieve this, we formulate the problem as a non-convex QP and attempt to locally maximize a measure (T-optimality condition) of the experiment's Fisher Information Matrix (FIM) under several constraints. These constraints include limits on the input amplitude, physiological output magnitude, subject control amplitude, and input signal autocorrelation. Because the autocorrelation constraint takes the form of a Quadratic Constraint (QC), we replace it with a conservative linear relaxation about a nominal point, which is iteratively updated during the course of optimization. We show that this *iterative descent algorithm generates a convergent sub-optimal solution that guarantees monotonic non-increasing of the cost function while satisfying all constraints during iterations. Finally, we present example experimental results using an optimized input sequence.*

1 INTRODUCTION

In recent years, clinical researchers have expanded the study of the human seated postural control system through the application of control theoretic analysis techniques [1, 2]. These studies often rely on accurate models of the underlying dynamics of the human in order to make the analysis tractable. However, humans possess a number of characteristics which may be impossible to measure accurately *a priori*, such as moments of inertia of body segments, center of mass (COM) locations, or feedback control gains. These parameters may instead be recoverable via examination of an experimental response. In the control sciences field, the set of techniques for recovering unknown or partially unknown model parameters from an experimental response are known as "system identification" techniques.

The design and optimization of system identification experiments is both a well-studied and ongoing problem in the literature [3–10]. Recent results in experimental optimization tend to favor the technique of optimizing the spectrum of the input signal [6–9]. This technique poses a number of challenges for human experiments. Human subjects tend to fatigue quickly during motor control testing, which limits the feasible length of each trial. This issue makes frequency-domain techniques for optimal experimental design difficult to use, because the time sequence may be too short to produce accurate results at low frequency or may not maintain sufficient frequency resolution over the entire spectrum. Thus, it would be preferable to design inputs in the time-domain (for short input sequences). Additionally, it is difficult to adapt frequency-domain optimization techniques to the number and variety of constraints within which an optimal solution for human testing must remain. For example, while it is obviously crucial to never apply enough force to a subject to cause injury, it is also important to make sure that the frequency characteristics of the input do not cause the subject to switch control strategies [11] (depending on the study goals). The input must not cause the subject's motion amplitude to grow large enough to cause injury. Finally, inputs given to human subjects must not become predictable enough for the subject to adopt a feedforward-type control strategy when only the feedback mechanisms are to be estimated, which is the case in this work.

In the time-domain, a problem which optimizes the information in an input sequence while satisfying the preceding constraints can be most readily formulated as a nonconvex Quadratically-Constrained Quadratic Program (QCQP), which tend to be NP-hard (Non-deterministic Polynomial-time hard) for many non-trivial problems [12]. While complete solutions to nonconvex QCQP's are not yet available, current techniques for solving or approximately solving these problems tend to exploit some combination of semi-definite relaxation, linear relaxation, or randomization [12, 13].

Our contributions in this work are as follows. We formulate a time-domain Quadratic Program (QP) designed to optimize the design of an experimental input for identification of parameters in a Linear Time-Invariant (LTI) human seated postural control model. In this approach, we maximize the trace of the experiment's Fisher Information Matrix (FIM), an objective known as T-optimality [14], while ensuring that the system does not violate a number of input and state constraints. Maximizing a measure of the FIM will improve the quality of the estimated parameters [15]. We formulate a novel quadratic constraint on the input sequence's autocorrelation function to ensure that the input is both unpredictable to subjects and possesses the desired frequency characteristics. By computing an iterative linear relaxation of this autocorrelation constraint, we are able to formulate the problem as a tractable nonconvex QCQP which can be solved locally at each iteration. We show that this iterative algorithm generates a convergent sub-optimal solution that guarantees monotonic non-increasing of the cost function while satisfying all constraints during iterations. Our approach is applied to optimize the design of a human seated balance identification experiment. We show simulation results for this design using model parameters derived from a preliminary set of subject parameters, and apply the optimized input to an experimental subject using a novel backdrivable robotic seat that we have developed. The experimental results demonstrate that we are able to reduce the variance of parameters recovered from an experiment using the optimized input versus parameters recovered from an experiment using a preliminary input of similar difficulty. A preliminary version of this paper without statistical experimental data was presented at the 2014 American Control Conference [16].

The rest of this paper is organized as follows: in Section 2, we present the dynamic model for the seated balance task. In Section 3, we derive the QP formulation for the experimental optimization and present the constraints under which the optimization will operate. In Section 4, we show results from an input optimization for one subject, and apply the optimized input to the subject. Finally, in Section 5, we offer some concluding remarks.

Standard notation will be used throughout the paper. Let $\mathbb{R}$, $\mathbb{R}_+$, and $\mathbb{B}$ denote, respectively, the sets of real, positive real, and binary (i.e. $\{0, 1\}$) numbers. The operators of expectation and covariance matrix are denoted by $\mathbb{E}$ and Cov, respectively. A random vector x, which has a multivariate normal distribution of mean vector μ and covariance matrix Σ, is denoted by $x \sim \mathcal{N}(\mu, \Sigma)$. An identity matrix of size $n \times n$ is denoted as I_n. A vector of zeros of length n is denoted as 0_n. The Kronecker product is denoted by the operator $\otimes$. The vectorization of a matrix A is denoted by $\mathrm{vec}(A)$. Other notation will be explained as it is used.

2 EXPERIMENTAL MODELING

We have developed a highly backdrivable torque-control robot that we intend to use for this and future studies on human seated postural control. This robot consists of a direct-drive backdrivable electric motor (CDDR C062C, Kollmorgen Inc.) coupled to a free-spinning seat platform (Fig. 4), displacement sensors in the motor, and a real-time electronic control unit (cRIO-9022, National Instruments Inc.). The motor is capable of providing peak torque inputs of up to 117 Nm. Since there is no gearbox or flexible coupling between the motor and seat, we can safely control the torque applied to the seat in a feedforward manner by specifying the motor current. This highly backdrivable configuration allows us to easily generate haptic effects (virtual springs, dampers, and other force fields) in addition to torque disturbances without needing direct torque measurements for feedback. Applying these effects through a direct-drive motor means that both stability and disturbance characteristics can be fine-tuned without physically reconfiguring the system and without needing to compensate for complicated gearbox effects (stiction, backdrivability, etc.) in the control algorithm. For safety purposes, the robot has mechanical stops at $\pm 15\,\mathrm{deg}$ ($\pm 0.26\ rad$) which prevent motions of the seat platform from exceeding this range. The combined seat and actuator, along with control hardware, we refer to as the "backdrivable robot".

Using this robot, we have designed a seated balance experiment based on the one performed in [1]. In the current experiment, the subject sits atop the backdrivable robotic seat which is free to pivot about an axis perpendicular to the coronal plane (Figs. 3 and 4). The angle of the lower body from vertical is α_1 and the angle of the upper body from vertical is α_2. Similar to the convention in [1], the portion of the subject and seat below the fourth lumbar ($L4$) vertebrae is lumped into a single rigid element with mass M_1 and moment of inertia (about the COM) of J_1. The COM is at a distance l_1 from the pivot point of the seat. Similarly, the portion of the subject above the $L4$ vertebrae is lumped into a rigid element with mass M_2 and moment of inertia J_2 about the COM. The COM of the upper body is a distance l_2 from the $L4$ vertebrae. The $L4$ vertebrae itself is at a distance l_{12} from the seat pivot. The human can apply a control torque u_h about the $L4$ vertebrae, and additionally possesses an intrinsic rotational stiffness k_h and intrinsic rotational damping c_h about $L4$. We apply (through feedback) a virtual stiffness k_r and a virtual damping c_r about the pivot point, in addition to a torque disturbance u. The sum of these torques produce the total robot torque u_r about the pivot point, i.e. $u_r = u - k_r\alpha_1 - c_r\dot{\alpha}_1$. The resulting dynamics can be determined by application of Lagrange's equation to the model in Fig. 3, resulting in the dynamic equations

$$\begin{aligned} u_r - u_h = {} & \ddot{\alpha}_1(J_1 + M_1 l_1^2 + M_2 l_{12}^2) \\ & + \ddot{\alpha}_2 M_2 l_{12} l_2 \cos(\alpha_1 - \alpha_2) \\ & + \dot{\alpha}_2^2 M_2 l_{12} l_2 \sin(\alpha_1 - \alpha_2) \\ & + c_h(\dot{\alpha}_1 - \dot{\alpha}_2) + k_h(\alpha_1 - \alpha_2) - M_1 g l_1 \sin\alpha_1 \\ & - M_2 g l_{12} \sin\alpha_1, \end{aligned} \tag{1}$$

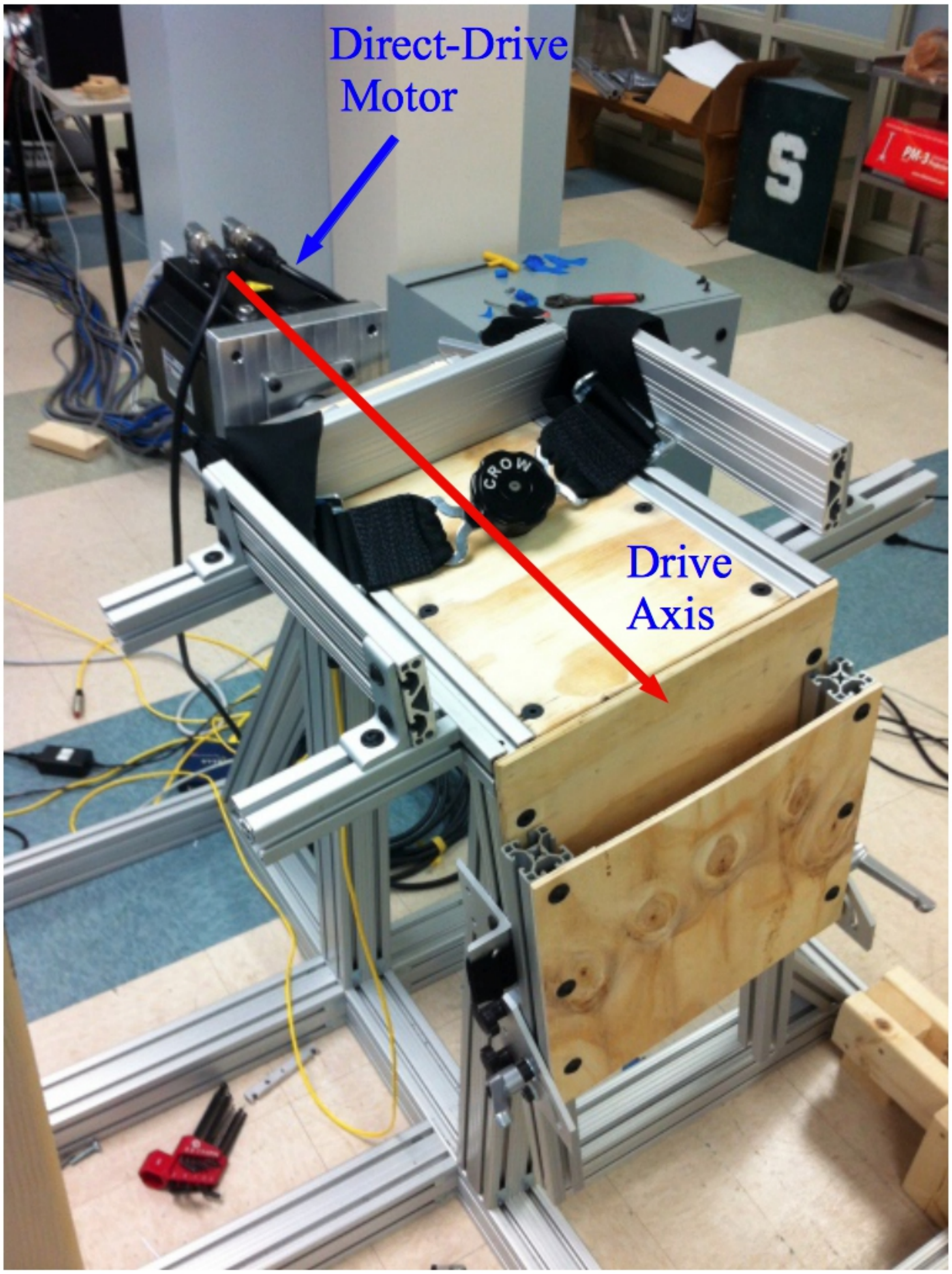

Figure 1: Experimental robot system, including backdrivable actuator and subject seat

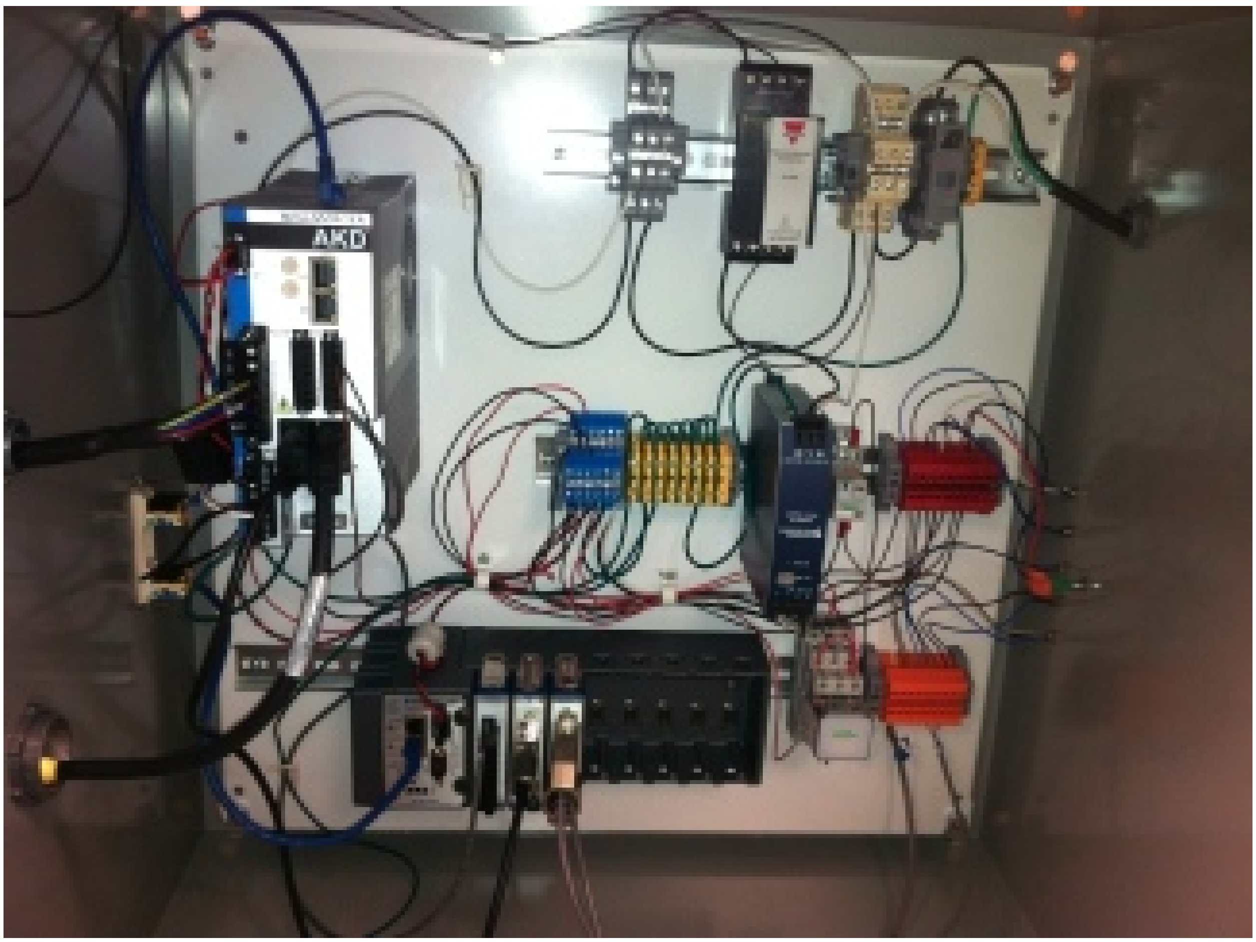

Figure 2: Real-time controller and motor amplifier for the compliant robot

and

$$
\begin{aligned}
u_h = {} & \ddot{\alpha}_2 (J_2 + M_2 l_2^2) \\
& + \ddot{\alpha}_1 M_2 l_{12} l_2 \cos(\alpha_1 - \alpha_2) \\
& - \dot{\alpha}_1^2 M_2 l_{12} l_2 \sin(\alpha_1 - \alpha_2) \\
& + c_h(\dot{\alpha}_2 - \dot{\alpha}_1) + k_h(\alpha_2 - \alpha_1) - M_2 g l_2 \sin\alpha_2,
\end{aligned}
\tag{2}
$$

with $g = 9.81\ m/s^2$ the acceleration due to gravity.

We model the closed-loop dynamical structure of the coupled human/backdrivable robot system as shown in Fig. 5. The plant model P represents the dynamics of the system in Eqns. (1) and (2) linearized about the upright equilibrium point. The first output $z = \begin{bmatrix} \alpha_1 & \dot{\alpha}_1 & \alpha_2 & \dot{\alpha}_2 \end{bmatrix}^T$ contains measurements of all the states of the system in Fig. 3 and is assumed to be exactly measurable by the human (via vestibular and proprioceptive mechanisms). The second output $z_r = \begin{bmatrix} \alpha_1 & \dot{\alpha}_1 \end{bmatrix}^T$ contains measurements of the subset of states (seat angle and rate) that are measurable by the robot via its displacement sensors.

There is a feedback controller R utilizing z_r such that the robot can simulate a desired dynamical system (in this case, a spring-damper system). The purpose of this controller is to slow the unstable poles of the closed-loop system enough for the system to be stabilizable by a human subject. Other studies of unstable seated balance commonly employ similar techniques, such as adding physical springs [17,18] or having the seat balance on a hemisphere instead of a point [1]. Our robot can additionally apply a torque disturbance u to the seat which can be used as an excitation signal for system identification [15]. Both of these signals are combined and converted into a torque through the robot motor M.

The model of the human has a feedback loop presumed to consist of a sensory delay $e^{-\tau s}$ implemented as a 5th-order Padé approximation, i.e.

$$
\begin{aligned}
e^{-\tau s} \approx {} & [30240 - 15120\tau s + 3360(\tau s)^2 - 420(\tau s)^3 \\
& + 30(\tau s)^4 - (\tau s)^5]/[30240 + 15120\tau s \\
& + 3360(\tau s)^2 + 420(\tau s)^3 + 30(\tau s)^4 + (\tau s)^5],
\end{aligned}
$$

and an output feedback controller K such that (if we ignore delays), the human control is $u_h = Kz$, where $K = \begin{bmatrix} -K_1 & -K_2 & -K_3 & -K_4 \end{bmatrix}$. We also include an approximation of

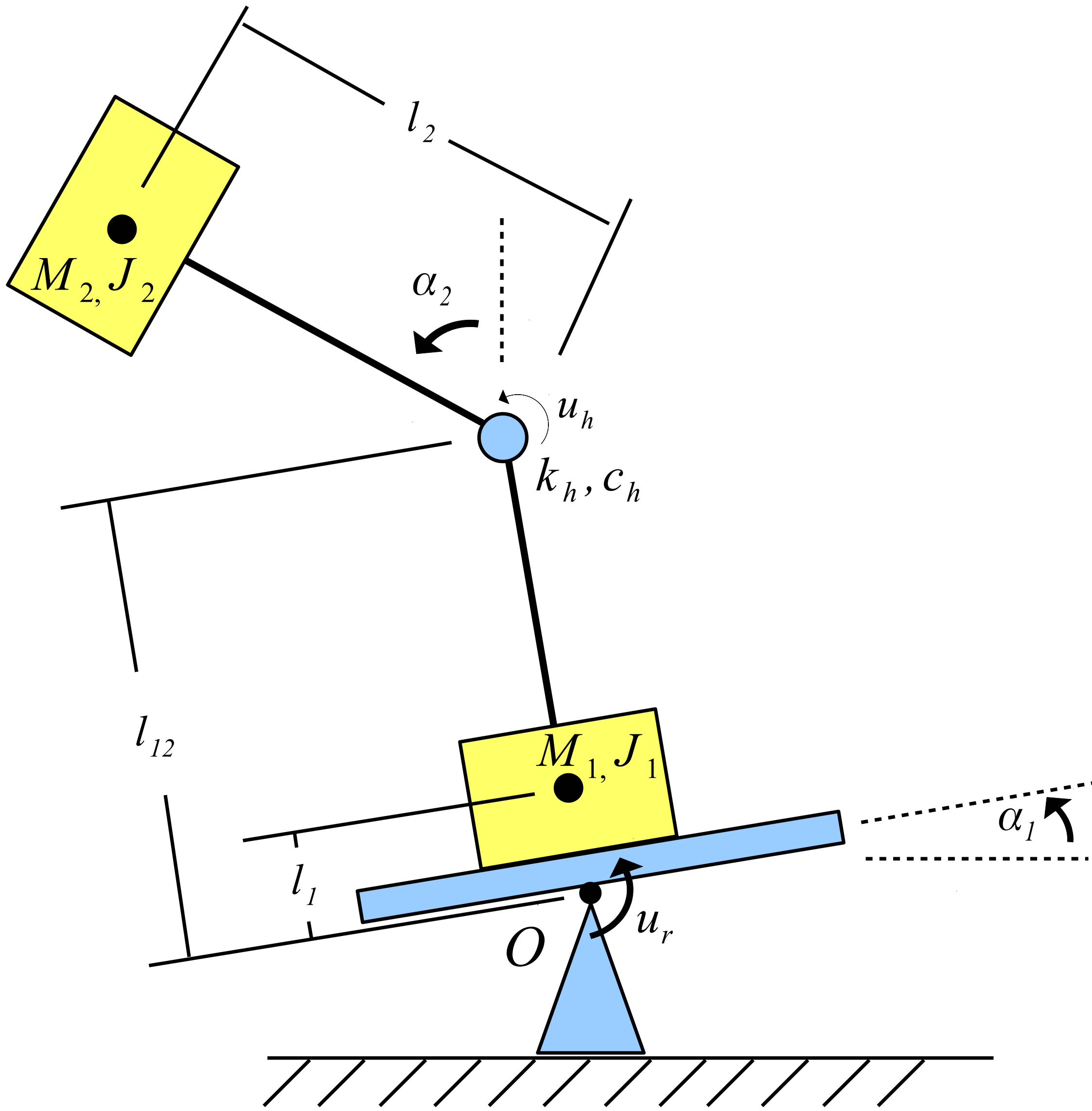

Figure 3: Simplified mechanical diagram of the seated balance experiment

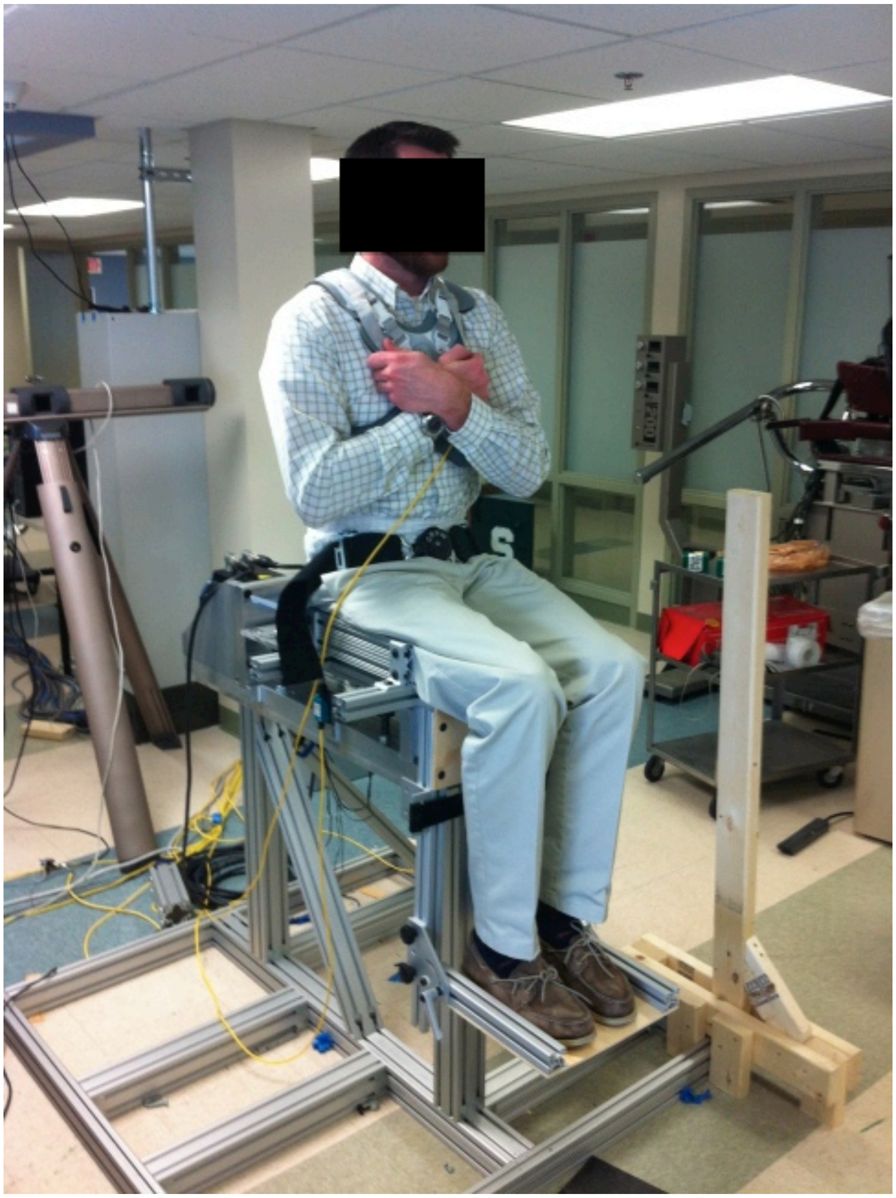

Figure 4: Subject on the backdrivable robot

muscle dynamics using a first-order filter with time constant T_ω. This formulation of the human feedback loop is similar to that used in other studies on postural control [1] and muscle control [19].

A motion capture system using LED markers is used to capture the upper and lower body angles for external processing (Visualeyez Motion Capture System, Phoenix Technologies Inc., Burnaby Canada). However, the angular rates $(\dot{\alpha}_1, \dot{\alpha}_2)$ are not directly measurable, so we reduce the plant output z to $y = \begin{bmatrix} \alpha_1 & \alpha_2 \end{bmatrix}^T$ via the operator D_y, i.e.

$$\begin{aligned} y &= \begin{bmatrix} 1 & 0 & 0 & 0 \\ 0 & 0 & 1 & 0 \end{bmatrix} z \\ &= D_y z. \end{aligned}$$

Additive white sensor noise w in the motion capture system is also presumed to exist.

A preliminary experiment was performed on a single subject in order to determine an initial parameter vector estimate $\hat{\theta}_0$ that could be used in subsequent optimizations. Because it only involved a single subject, this testing was designated as non-regulated research by the MSU Institutional Review Board (IRB). For this experiment, the virtual spring k_r and damper c_r were empirically tuned so that the subject needed to apply feedback to stabilize the seat, but did not tire excessively while maintaining upright balance. These values are listed in Table 1. 10 trials of 30 seconds duration were performed. During each trial, the subject was given an identical torque input u designed as a Pseudo-Random Binary Sequence (PRBS) with significant power only below approximately 1 Hz. A PRBS sequence was attractive for initial identification because it is in common use for system identification [15], and has spectral characteristics similar to the "reduced-power" input method [20] that has been used with success in human studies. The amplitude of this sequence was tuned to 6 Nm, which was the maximum amplitude that the subject could consistently stabilize for 30 seconds without the seat contacting the mechanical stops at ± 0.26 rad. The subject was given instructions to maintain stable upright posture on the seat while the perterbations were being applied. For each trial, the resulting angles α_1 and α_2 were measured using the motion capture system. "Successful" completion of a trial was defined as the subject being able to complete the entire 30 second trial without contacting the mechanical stops.

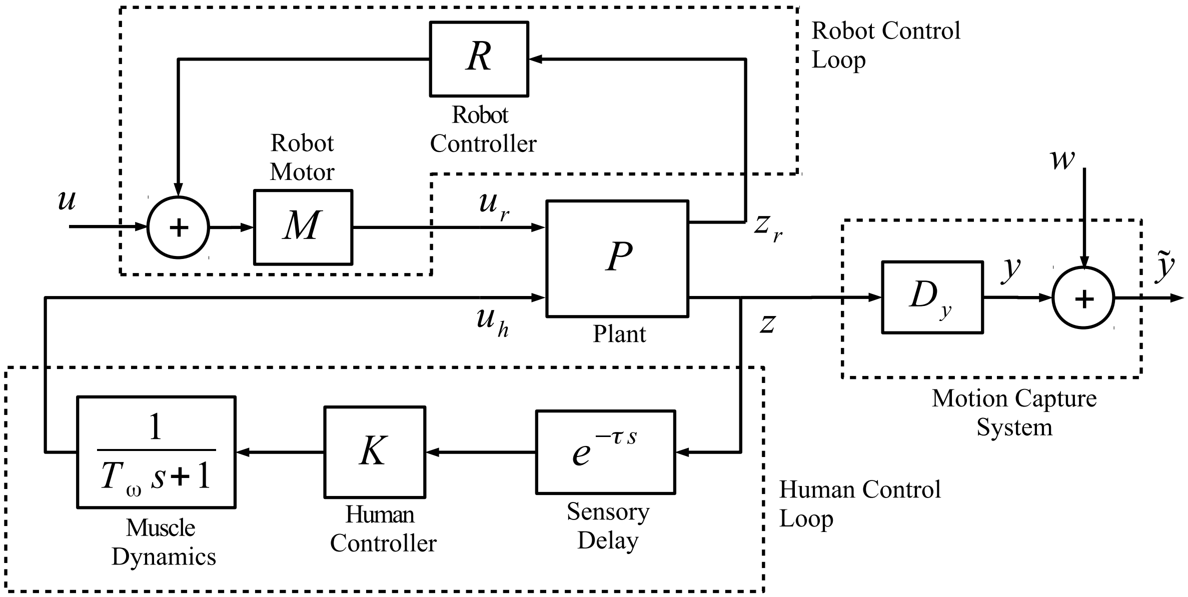

Figure 5: Block diagram of the seated balance experiment

We have determined a set of estimated model parameter values $\hat{\theta}_0$ for the subject through a combination of nonlinear least-squares fitting to this preliminary experiment, mean parameters fitted in a similar study [1], and tabulated data from subject height and weight [21] with $\theta := [K_1\ K_2\ K_3\ K_4\ J_1\ J_2\ l_1\ l_{12}\ l_2\ \tau\ T_\omega]^T$. The initial estimated values $\hat{\theta}_0$ of these parameters are listed above the double lines in Table 1, in addition to the fixed parameters below the double lines, which we assume can be recovered or specified for the system *a priori*.

3 EXPERIMENTAL OPTIMIZATION

3.1 Quadratic Program

Assume, for the moment, that the true parameter vector θ_0 is known. Because all of the subsystems are linear and rational-ordered, the closed-loop system in Fig. 5 with θ_0 known

Table 1: Initial estimated subject parameters $\hat{\theta}_0$ (above double lines) and fixed parameters (below double lines). The source of each parameter is given via the following labels: "LSQ" parameters were determined via least-squares fitting to the preliminary experiment, and are the mean of the values fitted in each of the 10 trials. "TAB" parameters were determined via applying the tables in [21]. Parameters labelled "SPEC" could be tuned and were specified prior to the experiment.

Parameter	Value	Source
K_1	143.55	LSQ
K_2	105.86	LSQ
K_3	677.98	LSQ
K_4	242.17	LSQ
J_1	2.026 $kg - m^2$	LSQ
J_2	2.988 $kg - m^2$	LSQ
l_1	0.0022 m	LSQ
l_{12}	0.245 m	LSQ
l_2	0.395 m	LSQ
τ	0.0252 s	LSQ
T_ω	0.0989	LSQ
M_1	55 kg	TAB
M_2	39.5 kg	TAB
k_r	100 Nm/rad	SPEC
c_r	2 Nms/rad	SPEC
k_h	13.15 Nm/rad	[1]
c_h	4.72 Nms/rad	[1]

can be formulated as a discrete-time LTI state-space model of the form

$$\begin{aligned} x_{k+1} &= A(\theta_0)x_k + B(\theta_0)u_k \\ y_k &= C(\theta_0)x_k \\ \tilde{y}_k &= C(\theta_0)x_k + w_k, \end{aligned} \tag{3}$$

with $x_k \in \mathbb{R}^{n_x}$, $u_k \in \mathbb{R}$, $y_k \in \mathbb{R}^{n_y}$, $w_k \sim \mathcal{N}(0, \Sigma) \in \mathbb{R}^{n_y}$ white and uncorrelated in time, $\theta \in \mathbb{R}^{n_\theta}$, and some sampling time T. The true parameter vector θ_0 is presumed to belong to a compact set Θ such that

$$\begin{aligned} \theta_0 \in \Theta = \{\rho \in \mathbb{R}^{n_\theta} \mid \rho_{i,min} \leq \theta_{0,i} \leq \rho_{i,max}\}, \\ \forall i = 1, \cdots, n_\theta. \end{aligned}$$

If the parameter vector θ_0 is known, then the matrices $A(\theta_0)$, $B(\theta_0)$, and $C(\theta_0)$ of the closed-loop model in (3) can be computed numerically using the MATLAB *connect* command (see Appendix A). The system is defined over the time indices $k \in \mathcal{K} := \{0, \cdots, N\}$ such that $t_k = kT$. We define the error e_k between the nominal output y_k and the noisy output $\tilde{y}_k$ for a given time index k and the true parameter vector θ_0 as

$$\begin{aligned} e_k(\theta_0) &:= \tilde{y}_k - y_k \\ &:= \tilde{y}_k - C(\theta_0)A(\theta_0)x_{k-1} - C(\theta_0)B(\theta_0)u_{k-1}. \end{aligned} \tag{4}$$

For the remainder of this paper, we will drop the explicit notational dependence on θ in A, B, and C.

Let us consider an experiment with an input sequence defined as $u := [u_0 \cdots u_{N-1}]^T$. Note that we can determine the system output y_k at an arbitrary time index $k \geq 1$ when the input sequence $[u_0, u_1, \cdots, u_{k-1}]^T$ and initial state condition x_0 are known. The complete solution to the discrete-time state-space system given in Eqn. (3) is

$$y_k = CA^k x_0 + C\sum_{i=0}^{k-1} A^{k-i-1}Bu_i.$$

Note that we can reconfigure this solution as a matrix operation:

$$y = \begin{bmatrix} y_1 \\ y_2 \\ \vdots \\ y_N \end{bmatrix} = \left[\begin{array}{c|cccc} CA & CB & \cdots & 0 \\ CA^2 & CAB & \cdots & 0 \\ \vdots & \vdots & \ddots & \vdots \\ CA^N & CA^{N-1}B & \cdots & CB \end{array}\right] \begin{bmatrix} x_0 \\ u_0 \\ \vdots \\ u_{N-1} \end{bmatrix} = GU.$$

We now have a non-recursive solution $y \in \mathbb{R}^{Nn_y}$ for all time $k \geq 1$ given $U \in \mathbb{R}^{N+n_x}$. Note that the first element in U is x_0. We can now define a vector form of the error $e = \tilde{y} - y = \begin{bmatrix} e_1^T & e_2^T & \cdots & e_N^T \end{bmatrix}^T \in \mathbb{R}^{Nn_y}$.

The log likelihood function for a data set $\tilde{y} := \begin{bmatrix} \tilde{y}_1^T & \cdots & \tilde{y}_N^T \end{bmatrix}^T$ given the true parametrization θ_0 is

$$\begin{aligned} \ln p(\tilde{y}|\theta_0) &= \sum_{k=1}^{N} \ln p(\tilde{y}_k|\theta_0) \\ &= -\frac{N}{2}\ln 2\pi - \frac{N}{2}\ln|\Sigma| \\ &\quad - \frac{1}{2}\sum_{k=1}^{N} e_k^T(\theta_0)\Sigma^{-1}e_k(\theta_0). \end{aligned}$$

The maximum likelihood estimator for θ_0 is then given by

$$\begin{aligned} \hat{\theta}_N &= \arg\min_{\theta\in\Theta} \left(\frac{1}{N}\sum_{k=1}^{N} e_k^T(\theta)\Sigma^{-1}e_k(\theta) \right), \\ &= \arg\min_{\theta\in\Theta} J_N(\theta). \end{aligned}$$

Under mild conditions [15, 22], it can be shown that

$$\lim_{N\to\infty} \hat{\theta}_N = \theta_0 = \arg\min_{\theta\in\Theta} \lim_{N\to\infty} \mathbb{E}\left\{J_N(\theta)\right\} \text{ w.p.1},$$

and that the prediction error converges in distribution to a normally distributed random variable [15, 22, 23]

$$\sqrt{N}\left(\hat{\theta}_N - \theta_0\right) \xrightarrow{d} \mathcal{N}\left(0, \mathbb{I}^{-1}(u;\theta_0)\right),$$

where $\mathbb{I}(u;\theta_0)$ is the FIM.

For a MIMO system, the FIM is an extension of the SISO case given in [24] and [25]:

$$\begin{aligned} \mathbb{I}(u;\theta_0) &= \mathbb{E}_{\tilde{y}|\theta_0}\left[\left(\left.\frac{\partial \ln p(\tilde{y}|\theta)}{\partial\theta}\right|_{\theta=\theta_0} \right) \left(\left.\frac{\partial \ln p(\tilde{y}|\theta)}{\partial\theta}\right|_{\theta=\theta_0} \right)^T \right] \\ &= \left[\sum_{k=1}^{N} \left(\left.\frac{\partial e_k}{\partial\theta}\right|_{\theta=\theta_0} \right)^T \Sigma^{-1} \left(\left.\frac{\partial e_k}{\partial\theta}\right|_{\theta=\theta_0} \right) \right]. \end{aligned}$$

Taking the partial of e_k with respect to the i^{th} element of θ yields

$$\frac{\partial e_k}{\partial\theta_i} = -\frac{\partial y_k}{\partial\theta_i}, \quad i = \left\{1, \cdots, n_\theta\right\}.$$

Then, we have

$$\left.\frac{\partial e}{\partial \theta_i}\right|_{\theta=\theta_0} = -\left.\frac{\partial y}{\partial \theta_i}\right|_{\theta=\theta_0} = -\left.\frac{\partial G}{\partial \theta_i}\right|_{\theta=\theta_0} U := -H_i U.$$

We can combine these matrices H_i for each θ_i to form

$$\mathcal{H} = \begin{bmatrix} H_1 & H_2 & \cdots & H_{n_\theta} \end{bmatrix} \in \mathbb{R}^{N n_y \times n_\theta (n_x + N)}.$$

Additionally, we form

$$\mathcal{U} = I_{n_\theta} \otimes U \in \mathbb{R}^{n_\theta (N + n_x) \times n_\theta}.$$

We can then form the FIM for the system in Eqn. (3) as

$$\mathbb{I}\left(u; \theta_0\right) = \left(\mathcal{H}\mathcal{U}\right)^T \left(I_N \otimes \Sigma^{-1}\right) \left(\mathcal{H}\mathcal{U}\right) \in \mathbb{R}^{n_\theta \times n_\theta}, \tag{5}$$

where all elements in $\mathcal{H}$ are assumed to be bounded, i.e., $\ell_{h1} \leq \mathcal{H}_{ij} \leq \ell_{h2}$. Note that the FIM is defined using the true parameter vector θ_0 [15]. However, in reality an optimization can only be performed based on the current best-estimate $\hat{\theta}_0$ [15]. Therefore, we will proceed from this point using $\hat{\theta}_0$ in place of θ_0.

Amongst a number of different optimality conditions [14], we choose the T-optimality condition, which will maximize the trace of the FIM [5, 26, 27], and in turn provides an objective that is quadratic in u. Because of the potentially large number of free variables in u, choosing a cost function that is purely quadratic in u will allow us to efficiently solve the problem using a QP algorithm later. We therefore use a cost $J(u; \hat{\theta}_0)$ defined by

$$J(u; \hat{\theta}_0) = -\text{trace}\left(\mathbb{I}(u; \hat{\theta}_0)\right). \tag{6}$$

Note that both the FIM and $J(u; \hat{\theta}_0)$ are functions of the input sequence u, the initial condition x_0, and estimated parameters $\hat{\theta}_0$ only. While the cost function $J(u; \hat{\theta}_0)$ is nonconvex in u [5], a general quadratic programming solver can be used to perform the unconstrained local minimization

$$u^\star = \arg\min_u J(u; \hat{\theta}_0). \tag{7}$$

3.2 Design Constraints

In this paper, the quadratic optimization in Eqns. (6)-(7) is subject to the following constraints:

- **Input Limits.** Since the direct-drive motor should be restricted to only apply a safe amount of torque, we apply a constraint such that

$$-u_m \leq u \leq u_m, \quad u_m \in \mathbb{R}_+.$$

- **Output Constraints.** There is a finite angular range over which both the robot seat platform and the human torso can move. We therefore apply the constraint

$$-1^N \otimes y_m \leq GU \leq 1^N \otimes y_m,$$

where 1^N is a vector of ones of length N, and $y_m \in \mathbb{R}_+^p$ defines the maximum amplitude of each output individually. Additionally, the angular difference $\tilde{\alpha} = \alpha_2 - \alpha_1$ is limited by both the structure and flexibility of the subject's lower back. By reformulating the closed-loop system in Fig. 5, we can form a structure G_δ similar to G where u is the input and $\tilde{\alpha}$ is the output. If $\hat{\theta}_0$ is known, then this reformulation can be performed numerically in MATLAB using *connect* (see Appendix A). We then apply the constraint

$$-\delta_\alpha \leq G_\delta U \leq \delta_\alpha, \quad \delta_\alpha \in \mathbb{R}_+.$$

- **Human Control Constraint.** The human subject is only capable of generating a finite amount of torque u_h. We can again reformulate the closed-loop system in Fig. 5 to form a structure G_u similar to G where u is the input and u_h is the output. Then, we apply the constraint

$$-u_{hm} \leq G_u U \leq u_{hm}, \quad u_{hm} \in \mathbb{R}_+.$$

- **Autocorrelation Constraint.** In addition to the preceding linear constraints, it was desired to constrain the autocorrelation of the input sequence so as to reduce predictability of the signal while maintaining desirable spectral characteristics. The autocorrelation of a discrete real time sequence u_k at lag j can be computed as

$$R_{uu}(u; j) = \sum_k u_k u_{k-j}.$$

We can reformulate this as the quadratic matrix multiplication

$$R_{uu}(u;j) = u^T Q(j) u, \tag{8}$$

where $Q(j) \in \mathbb{B}^{N \times N}$ is a Toeplitz matrix containing ones on its j^{th} upper off-diagonal and zeros everywhere else, e.g.

$$R_{uu}(u;1) = u^T \begin{bmatrix} 0 & 1 & 0 & \cdots & 0 \\ 0 & 0 & 1 & \cdots & 0 \\ \vdots & & \ddots & & \vdots \\ 0 & 0 & 0 & \cdots & 1 \\ 0 & 0 & 0 & \cdots & 0 \end{bmatrix} u.$$

We consider the term $R_{uu}(u)$ (with j ommitted) to be the autocorrelation vector for all lags $j = \left\{0, \cdots, \frac{N}{2} - 1\right\}$.

We desired the normalized autocorrelation of the first $N/2$ lags of the optimal input sequence autocorrelation to be within some region of our preliminary experiment's PRBS signal autocorrelation $R^{\star}_{uu}$, i.e.

$$R^{\star}_{uu} - \beta \leq \frac{R_{uu}(u)}{R_{uu}(u;0)} \leq R^{\star}_{uu} + \beta, \tag{9}$$

where $\beta > 0$ is a scalar constant. The constraint in (9) is quadratic in u based on the definition of $R_{uu}(u;j)$ in (8).

Unfortunately, the optimization of $J(\theta_0; u)$ subject to the constraints listed above is a nonconvex QCQP, the solution of which is still an open research question. Therefore, we propose an iterative linearization technique to find a good solution to Eqn. (7) in the next section.

3.3 Proposed Iterative Descent Algorithm

Since we can not directly apply a quadratic constraint such as the one in Eqn. (9) to the quadratic program, we propose to compute a linear relaxation of the autocorrelation about a nominal vector $\hat{u}$. This relaxation takes the form of a linearization based on a Taylor series expansion about $\hat{u}$, i.e.

$$\hat{R}_{uu}(\hat{u}; u; j) = \hat{u}^T Q(j) \hat{u} + \hat{u}^T \left(Q(j) + Q^T(j) \right) (u - \hat{u}) \,.$$

This constraint is made slightly more conservative than the true quadratic constraint in Eqn. (9) by shrinking the constraint boundary, i.e.

$$R^\star_{uu} - \beta + \gamma \leq \frac{\hat{R}_{uu}(\hat{u}; u)}{\hat{R}^0_{uu}} \leq R^\star_{uu} + \beta - \gamma, \tag{10}$$

where γ s.t. $0 < \gamma < \beta$ is a small constant. Note that we normalize $\hat{R}_{uu}(\hat{u}; u)$ by $\hat{R}^0_{uu}$, which we define as $\hat{R}^0_{uu} := R_{uu}(\hat{u}; 0)$. Now, by ensuring that $\tilde{u} = u - \hat{u}$ is constrained to be small, a local solution can be found that satisfies the linear constraint in Eqn. (10) but does not violate the quadratic autocorrelation constraint Eqn. (9).

To ensure that the linearization in Eqn. (10) is both always valid and more conservative than the true quadratic constraint Eqn. (9), we constrain the difference $\tilde{u} = u - \hat{u}$ such that

$$-\delta_u \leq \tilde{u} \leq \delta_u, \quad \delta_u \in \mathbb{R}^+. \tag{11}$$

Therefore, when we allow only a small change in u, we may solve the following optimization:

$$u^\star = \arg\min_u J(u; \theta_0), \tag{12}$$

subject to the constraints

$$\begin{aligned}
-u_m &\leq u \leq u_m, \\
-1^N \otimes y_m &\leq GU \leq 1^N \otimes y_m, \\
-\delta_\alpha &\leq G_\delta U \leq \delta_\alpha, \\
-u_{hm} &\leq G_u U \leq u_{hm}, \\
R^\star_{uu} - \beta + \gamma &\leq \frac{\hat{R}_{uu}(\hat{u}; u)}{\hat{R}^0_{uu}} \leq R^\star_{uu} + \beta - \gamma, \\
-\delta_u &\leq \tilde{u} \leq \delta_u.
\end{aligned} \tag{13}$$

An overall solution is found by computing a series of successive solutions $u^{\star i}$ to the problem of Eqn. (12) subject to the constraints in Eqn. (13). For each iteration i, we perform a local linearization Eqn. (10) of the quadratic autocorrelation constraint in Eqn.

Table 2: Iterative descent algorithm for optimization of the input sequence u

Input: (1) The estimated parameter vector $\hat{\theta}_0$

(2) The initial nominal input sequence $\hat{u}$

(3) The desired relative stopping tolerance E_{stop}

Output: (1) The optimal input vector $u^\star$

Build A, B, and C from $\hat{\theta}_0$

Compute G, G_δ, G_u, $\mathcal{H}$

Let $E > E_{\text{stop}}$

Let $i = 1$

while $E > E_{\text{stop}}$ **do**

  Compute $\hat{R}^0_{uu} = R_{uu}(\hat{u}, 0)$

  Assemble $U = \left[x_0^T u^T\right]^T$

  Assemble $\mathbb{I}\left(u; \hat{\theta}_0\right) = (\mathcal{H}\mathcal{U})^T \left(I_N \otimes \Sigma^{-1}\right)(\mathcal{H}\mathcal{U})$

  Solve for $u^{\star i}$ and $J(u^{\star i}; \hat{\theta}_0)$ from the QP in Eqn. (12), subject to the constraints in Eqn. (13)

  Let $E = \left|\frac{J(u^{\star i};\hat{\theta}_0) - J(u^{\star(i-1)};\hat{\theta}_0)}{J(u^{\star(i-1)};\hat{\theta}_0)}\right|$

  Let $\hat{u} = u^{\star i}$

  Let $i = i + 1$

end while

Let $u^\star = u^{\star i}$

(9) about $\hat{u} = u^{\star(i-1)}$ and solve for $u^{\star i}$. Each solution $u^{\star i}$ becomes $\hat{u}$ in the next iteration of the solution. This is done so as to allow u to traverse a wide range while not violating the input linearization constraint in Eqn. (11) at any point during the optimization. Each solution $u^{\star i}$ is found using MATLAB's *quadprog* general quadratic programming solver in combination with the *yalmip* modeling toolbox. Details of the solution procedure are shown in Table 2.

Note that we are computing the optimization based on the estimate $\hat{\theta}_0$, instead of the true parameter vector θ_0. This is a common problem in system identification, and can be dealt with via a number of methods, such as iterative system identification techniques [28].

3.4 Convergence Analysis

In this section, we discuss the convergence properties of the proposed iterative descent algorithm proposed in Table 2.

First note that $J(u^{\star i}; \hat{\theta}_0) \geq J(u^{\star i+1}; \hat{\theta}_0)$ by the construction. Next we show that J has a lower bound. This can be shown by the fact that the FIM in Eqn. (5) has an upper bound with an assumption that all elements in $\mathcal{H}$ are bounded, i.e., $\ell_{h1} \leq \mathcal{H}_{ij} \leq \ell_{h2}$. This follows from the fact that

$$\begin{aligned} \operatorname{trace}\left(\mathbb{I}\left(u; \hat{\theta}_0\right)\right) &= \operatorname{trace}\left(I_N \otimes \Sigma^{-1} \mathcal{H} \mathcal{U} \mathcal{U}^T \mathcal{H}^T\right) \\ &= \operatorname{vec}(I_N \otimes \Sigma^{-1})^T \operatorname{vec}(\mathcal{H} \mathcal{U} \mathcal{U}^T \mathcal{H}^T) \leq \ell_T, \end{aligned} \tag{14}$$

since all elements in $\mathcal{U}$ are also bounded due to the input constraints in the constrained optimization in Eqn. (12).

Since the value J has a lower bound which is $-\ell_T$ from Eqn. (14) and is monotonically non-increasing during the iterations, it will converge to some value as iterations proceed.

Therefore, this iterative descent algorithm generates a convergent sub-optimal solution that guarantees monotonic non-increasing of the cost function while satisfying all constraints during iterations.

4 CASE STUDY

We have performed a case study on a single subject to demonstrate our experimental optimization. The goal of the optimization is to determine an experimental input sequence that will minimize a measure of the covariance for the estimated parameters. This is achieved via a maximization of the experiment's FIM trace subject to constraints as described in (12)-(13). Using parameters $\hat{\theta}_0$ from Table 1, G, G_u, and G_δ from Sec. 3 were computed numerically using MATLAB's *connect* function (numerical values listed in Appendix B). The limits applied to the optimization are listed, along with their sources, in Table 3. We let $x_0 = \begin{bmatrix} 0.01 & 0_9^T \end{bmatrix}^T$, and since the sensor noise for both elements of y_k were approximately equal and uncorrelated, we let $\Sigma = I$. The initial input $\hat{u}$ was the same PRBS signal given to the subject in the preliminary experiment. Note that, in the preliminary experiment,

Table 3: Limits used for the optimization procedure. The values of y_m and δ_α are based on the maximum simulated displacements that occurred during fitting to the preliminary experiment. u_m is the maximum torque input level the subject found comfortable. u_{hm} is approximately half of the near-maximal lateral bending torque reported by male subjects in [29]. β, γ, and δ_u were tuned.

Limit	Value
u_m	$20\ Nm$
y_m	$\begin{bmatrix} 0.192 \\ 0.078 \end{bmatrix}\ rad$
δ_α	$0.252\ Nm$
u_{hm}	$60\ Nm$
β	0.16
γ	0.08
δ_u	$0.05\ Nm$

the initial $\hat{u}$ was challenging enough that the subject required considerable practice to complete the trials successfully (defined as no contact occurring with the mechanical stops at $\alpha_1 = \pm 0.26\ rad$ on the device.)

The descent algorithm in Algorithm 2 was applied using the initial parameter vector $\hat{\theta}_0$ from Table 1 and the initial PRBS input $\hat{u}$. For an input sequence with length $N = 300$ and a sampling time of $T = 0.1$ seconds, we were able to converge to a local suboptimal input sequence ($E_{\text{stop}} = 1 \times 10^{-3}$) in approximately 3.5 hours on a 2.2GHz Xeon server.

4.1 Optimization Results

The optimal input $u^\star$ along with the change in the objective function with increasing i are shown in Fig. 6. We simulate the system in Fig. 5 with $u(t) = u^\star$ to produce the corresponding outputs y and differential angle $\tilde{\alpha}$ (Fig. 7). The final signal autocorrelation $R^\star_{uu}$ and its constraints are also shown in Fig. 7. None of the other constraints for the system were active. The solution $u^\star$ produces an approximately 1.6 times improvement relative to the initial $\hat{u}$ in the value of the objective function without violating any of the

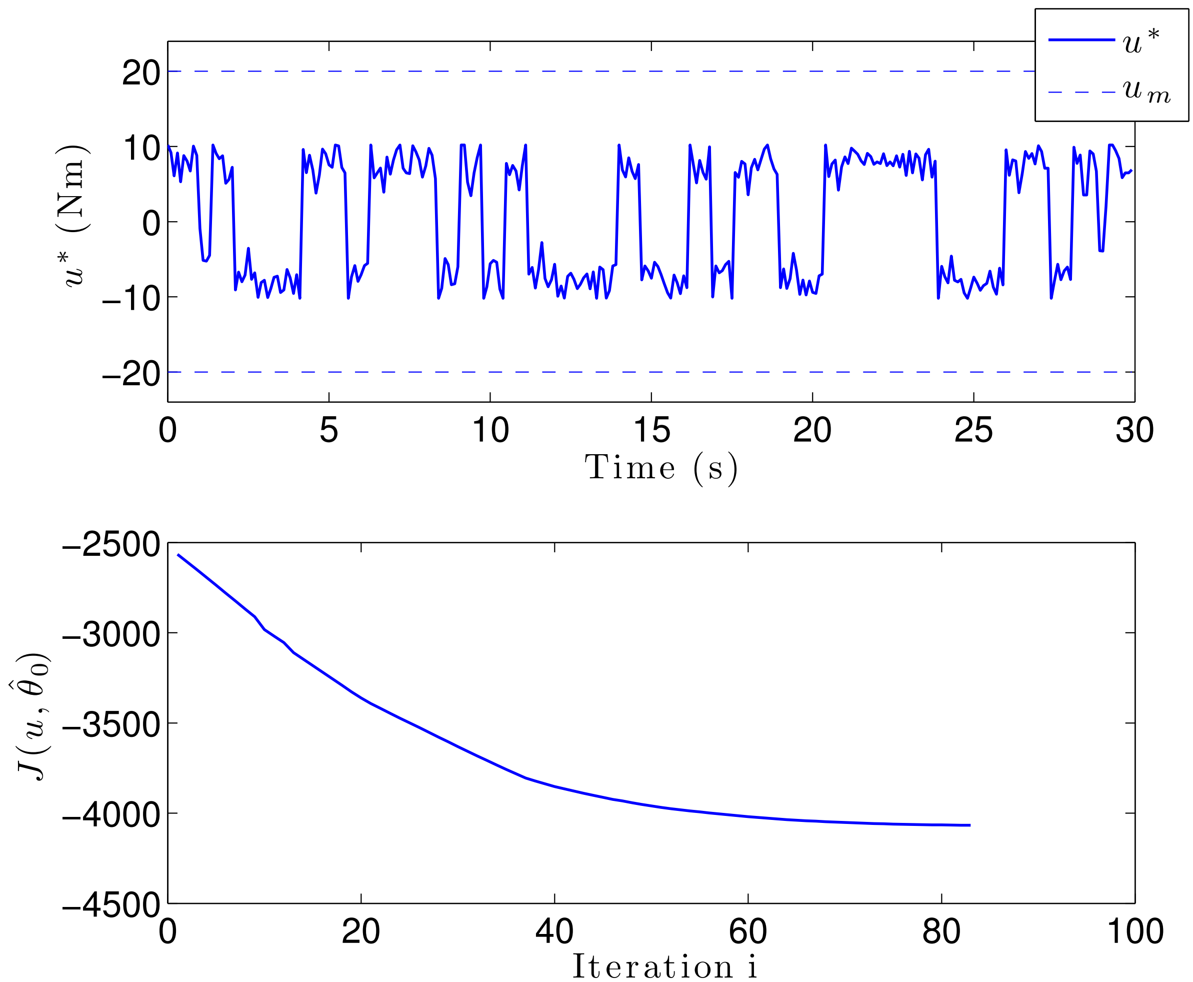

Figure 6: The upper plot shows the optimal input sequence $u^{\star}$. The lower plot shows the change in the objective function $J(u; \hat{\theta}_0)$ with increasing iteration i.

listed constraints.

4.2 Experimental Application

To compare the variance of the parameters fitted using the optimal experiment, we performed an experiment using the same subject tested in Sec. 2. This experiment was again designated as non-regulated research by the MSU IRB. 10 trials of the 30 seconds length using the optimal input $u^{\star}$ were performed using an experimental setup otherwise identical to that in Sec. 2. The subject was able to successfully complete the 10 trials of the experiment (no

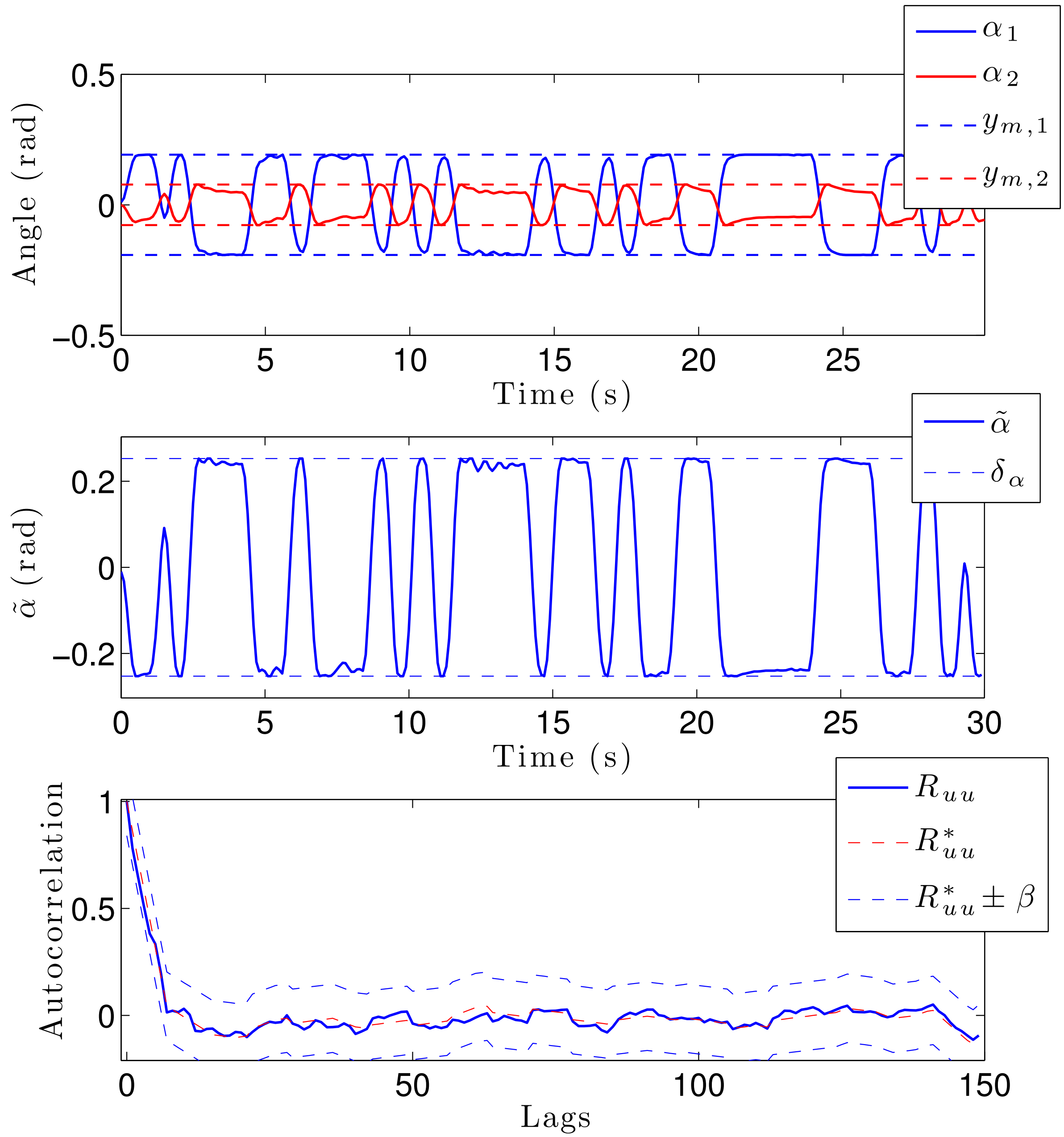

Figure 7: Simulated results using the optimal input $u^\star$. The upper plot shows the simulated angles α_1 and α_2 versus time, along with their bounds. The center plot shows the differential angle $\tilde{\alpha}$ versus time along with its bounds. The bottom plot shows the optimal input signal autocorrelation $R^\star_{uu}$ along with its bounds, and the original signal autocorrelation R_{uu} for comparison. The constraints on u_h were not active during simulation.

Table 4: Mean best-fit parameters $\hat{\theta}_N$ based on the optimal experiment. Fixed parameters are the same as those given in Table 1.

Parameter	Value
K_1	270.31
K_2	130.64
K_3	803.28
K_4	224.30
J_1	$3.060\ kg - m^2$
J_2	$2.925\ kg - m^2$
l_1	$0.0104\ m$
l_{12}	$0.2501\ m$
l_2	$0.3684\ m$
τ	$0.0368\ s$
T_ω	0.0315

mechanical stop contact), although the subjective difficulty of the the task was very high. The resulting mean best-fit parameters $\hat{\theta}_N$ are shown in Table 4, and in general match well with the parameters found in Table 1.

In Table 5, we compare the variance across 10 trials of the parameters fitted in the preliminary experiment done in Sec. 2 with the parameters fitted from the optimal experiment. It can be seen that, for almost all parameters, the optimal experiment reduced the variance of the resulting fitted parameters compared to the initial PRBS input while the mean values from the two estimators are similar.

Because the sequence $u^\star$ is only optimal for a parameter vector $\hat{\theta}_0$, in theory, this technique could be employed as part of a broader iterative procedure [28]. After a $u^\star$ is found, a subject can be tested using $u^\star$ as the input and the resulting experimental response fitted to find $\hat{\theta}_N$. The parameters $\hat{\theta}_N$ can then be fed back as $\hat{\theta}_0$ in the next iteration of the input optimization and the process repeated until a desired level of convergence is achieved [28].

Table 5: Variance of the parameters in $\hat{\theta}_0$ vs the variance of the parameters in $\hat{\theta}_N$.

Parameter	$\hat{\theta}_0$ Variance	$\hat{\theta}_N$ Variance
K_1	2727	2238
K_2	2374	496.6
K_3	5.306×10^4	5840
K_4	1.621×10^4	1238
J_1	1.031	0.2304
J_2	0.228	0.298
l_1	0.0007639	0.0005456
l_{12}	0.0008781	0.001225
l_2	0.004951	0.0009266
τ	0.0004225	0.000375
T_ω	0.005771	0.0004575

5 CONCLUSIONS

In this work, we have demonstrated a QP technique for generating an optimal experimental input for a human seated postural control identification experiment. To this end, we have formulated a quadratic objective function based on a measure of the FIM that will maximize the information present in the experiment for the proposed testing. This optimized input was designed to minimize the variance of the parameters recovered from the human subject. We have formulated a set of output, input, and control constraints, in addition to a unique linearized autocorrelation constraint, such that the resulting input signal will be feasible for the proposed testing. The resulting solution $u^\star$ converged to a local solution without violating any of the prescribed constraints. We have additionally demonstrated an experimental application of this input signal in conjunction with our backdrivable robot and shown that the resulting recovered parameters from the subject have lower variance than those recovered from a preliminary experiment, which is consistent with the goal of our optimization.

In future work, we intend to apply this technique in quantitative clinical testing, and extend our formulation to produce input sequences that guarantee a minimum level of performance across a subject population.

ACKNOWLEDGMENT

This work has been supported in part by grant number U19 AT006057 from the National Center for Complementary and Alternative Medicine (NCCAM) at the National Institutes of Health.

References

[1] Reeves, N. P., Cholewicki, J., and Narendra, K. S., 2009. "Effects of reflex delays on postural control during unstable seated balance". *Journal of biomechanics,* **42**(2), pp. 164–170.

[2] Xu, Y., Choi, J., Reeves, N., and Cholewicki, J., 2010. "Optimal control of the spine system". *Journal of biomechanical engineering,* **132**, p. 051004.

[3] Kiefer, J., 1959. "Optimum experimental designs". *Journal of the Royal Statistical Society. Series B (Methodological)*, pp. 272–319.

[4] Levadi, V., 1966. "Design of input signals for parameter estimation". *IEEE Transactions on Automatic Control,* **11**(2), pp. 205–211.

[5] Mehra, R., 1974. "Optimal input signals for parameter estimation in dynamic systems–survey and new results". *IEEE Transactions on Automatic Control,* **19**(6), pp. 753–768.

[6] Yuan, Z.-D., and Ljung, L., 1985. "Unprejudiced optimal open loop input design for identification of transfer functions". *Automatica,* **21**(6), pp. 697–708.

[7] Gevers, M., and Ljung, L., 1986. "Optimal experiment designs with respect to the intended model application". *Automatica,* **22**(5), pp. 543–554.

[8] Forssell, U., and Ljung, L., 2000. "Some results on optimal experiment design". *Automatica,* **36**(5), pp. 749–756.

[9] Jansson, H., and Hjalmarsson, H., 2005. "Input design via lmis admitting frequency-wise model specifications in confidence regions". *IEEE Transactions on Automatic Control,* **50**(10), pp. 1534–1549.

[10] Bombois, X., Scorletti, G., Gevers, M., Van den Hof, P. M., and Hildebrand, R., 2006. "Least costly identification experiment for control". *Automatica,* **42**(10), pp. 1651–1662.

[11] Forbes, P. A., de Bruijn, E., Schouten, A. C., van der Helm, F. C., and Happee, R., 2013. "Dependency of human neck reflex responses on the bandwidth of pseudorandom anterior-posterior torso perturbations". *Experimental brain research,* **226**(1), pp. 1–14.

[12] Luo, Z.-q., Ma, W.-k., So, A.-C., Ye, Y., and Zhang, S., 2010. "Semidefinite relaxation of quadratic optimization problems". *IEEE Signal Processing Magazine,* **27**(3), pp. 20–34.

[13] d'Aspremont, A., and Boyd, S., 2003. Relaxations and randomized methods for non-convex QCQPs. Tech. rep., Stanford University. EE392 Class Notes.

[14] Pukelsheim, F., 1993. *Optimal design of experiments*, Vol. 50. SIAM.

[15] Ljung, L., 1999. *System identification: theory for the user.* PTR Prentice Hall, Upper Saddle River, NJ.

[16] Priess, M., Choi, J., Radcliffe, C., Jr., J. P., Cholewicki, J., and Reeves, N., 2014. "Time-domain optimal experimental design in human postural control testing". In Proceedings of the 2014 IEEE American Control Conference.

[17] Lee, H., Granata, K. P., and Madigan, M. L., 2008. "Effects of trunk exertion force and direction on postural control of the trunk during unstable sitting". *Clinical Biomechanics,* **23**(5), pp. 505–509.

[18] Slota, G. P., Granata, K. P., and Madigan, M. L., 2008. "Effects of seated whole-body vibration on postural control of the trunk during unstable seated balance". *Clinical Biomechanics,* **23**(4), pp. 381–386.

[19] Prochazka, A., Gillard, D., and Bennett, D. J., 1997. "Implications of positive feedback in the control of movement". *Journal of neurophysiology,* **77**(6), pp. 3237–3251.

[20] Mugge, W., Abbink, D., and Van der Helm, F., 2007. "Reduced power method: how to evoke low-bandwidth behaviour while estimating full-bandwidth dynamics". In IEEE 10th International Conference on Rehabilitation Robotics, 2007., IEEE, pp. 575–581.

[21] Zatsiorsky, V. M., 2002. *Kinetics of human motion*. Human Kinetics.

[22] Hjalmarsson, H., 2005. "From experiment design to closed-loop control". *Automatica,* **41**(3), pp. 393–438.

[23] Aguero, J., and Goodwin, G. C., 2006. "On the optimality of open and closed loop experiments in system identification". In 45th IEEE Conference on Decision and Control, IEEE, pp. 163–168.

[24] Goodwin, G. C., and Payne, R. L., 1977. *Dynamic system identification: experiment design and data analysis*. Academic press.

[25] Rojas, C. R., Welsh, J. S., Goodwin, G. C., and Feuer, A., 2007. "Robust optimal experiment design for system identification". *Automatica,* **43**(6), pp. 993–1008.

[26] Aoki, M., and Staley, R., 1970. "On input signal synthesis in parameter identification". *Automatica,* **6**(3), pp. 431–440.

[27] Nahi, N., and Napjus, G., 1971. "Design of optimal probing signals for vector parameter estimation". In 1971 IEEE Conference on Decision and Control, Vol. 10, IEEE, pp. 162–168.

[28] Schrama, R. J., 1992. "Accurate identification for control: The necessity of an iterative scheme". *IEEE Transactions on Automatic Control,* **37**(7), pp. 991–994.

[29] McGill, S. M., 1992. "A myoelectrically based dynamic three-dimensional model to predict loads on lumbar spine tissues during lateral bending". *Journal of biomechanics,* **25**(4), pp. 395–414.

Appendix A

```
function dsys0=buildsys(params,flag)

J1=params.J1;
J2=params.J2;
M1=params.M1;
M2=params.M2;
l1=params.l1;

l12=params.l12;

l2=params.l2;
kr=params.kr;
cr=params.cr;
g=params.g;
kh=params.kh;
ch=params.ch;
K1=params.K1;
K2=params.K2;
K3=params.K3;
K4=params.K4;

delay=params.delay;
tc=params.tc;
T=params.T;




Ap=[ 0, 1, 0,0;...
 -(J2*kh + J2*kr + M2*kh*l2^2 + M2*kr*l2^2 - M2^2*g*l12*l2^2 ...
   - J2*M1*g*l1 - J2*M2*g*l12 + M2*kh*l12*l2 - M1*M2*g*l1*l2^2)...
    /(M1*M2*l1^2*l2^2 + J2*M1*l1^2 + J2*M2*l12^2 + J1*M2*l2^2 + J1*J2),...
```

```
    -(J2*ch + J2*cr + M2*ch*l2^2 + M2*cr*l2^2 + M2*ch*l12*l2)...
    /(M1*M2*l1^2*l2^2 + J2*M1*l1^2 + J2*M2*l12^2 + J1*M2*l2^2 + J1*J2),...
    (- g*l12*M2^2*l2^2 + kh*M2*l2^2 + kh*l12*M2*l2 + J2*kh)...
    /(M1*M2*l1^2*l2^2 + J2*M1*l1^2 + J2*M2*l12^2 + J1*M2*l2^2 + J1*J2),...
    (M2*ch*l2^2 + M2*ch*l12*l2 + J2*ch)/(M1*M2*l1^2*l2^2 + J2*M1*l1^2 ...
                                    + J2*M2*l12^2 + J1*M2*l2^2 + J1*J2);...
  0, 0,0,1;...
  (J1*kh + M1*kh*l1^2 + M2*kh*l12^2 - M2^2*g*l12^2*l2 + M2*kh*l12*l2 ...
   + M2*kr*l12*l2 - M1*M2*g*l1*l12*l2)...
    /(M1*M2*l1^2*l2^2 + J2*M1*l1^2 + J2*M2*l12^2 + J1*M2*l2^2 + J1*J2),...
    (J1*ch + M1*ch*l1^2 + M2*ch*l12^2 + M2*ch*l12*l2 + M2*cr*l12*l2)...
    /(M1*M2*l1^2*l2^2 + J2*M1*l1^2 + J2*M2*l12^2 + J1*M2*l2^2 + J1*J2),...
    -(- g*l2*M2^2*l12^2 - M1*g*l2*M2*l1^2 + kh*M2*l12^2 + kh*l2*M2*l12 ...
      - J1*g*l2*M2 + M1*kh*l1^2 + J1*kh)...
    /(M1*M2*l1^2*l2^2 + J2*M1*l1^2 + J2*M2*l12^2 + J1*M2*l2^2 + J1*J2),...
    -(M1*ch*l1^2 + M2*ch*l12^2 + M2*ch*l2*l12 + J1*ch)/(M1*M2*l1^2*l2^2 ...
    + J2*M1*l1^2 + J2*M2*l12^2 + J1*M2*l2^2 + J1*J2)];

Bp=[ 0, 0;...
 (M2*l2^2 + J2)/(M1*M2*l1^2*l2^2 + J2*M1*l1^2 + J2*M2*l12^2 + J1*M2*l2^2 + J1*J2),...
    -(M2*l2^2 + M2*l12*l2 + J2)/(M1*M2*l1^2*l2^2 + J2*M1*l1^2 + J2*M2*l12^2 + J1*M2*l2^2 +
     0,0;...
   -(M2*l12*l2)/(M1*M2*l1^2*l2^2 + J2*M1*l1^2 + J2*M2*l12^2 + J1*M2*l2^2 + J1*J2),...
    (M1*l1^2 + M2*l12^2 + M2*l2*l12 + J1)/(M1*M2*l1^2*l2^2 + J2*M1*l1^2 + J2*M2*l12^2 + J1

Cp=eye(4);
Dp=zeros(4,2);

Plant=ss(Ap,Bp,Cp,Dp);
Plant.inputname={'taur','tauh'};
Plant.outputname={'y1','y2','y3','y4'};


Ksys=ss(0,zeros(1,4),0,-[K1 K2 K3 K4]);
Ksys.inputname={'y1','y2','y3','y4'};
Ksys.outputname='Kout';
```

```
[n,d]=pade(delay,5);
delaysys=tf(n,d);
delaysys.inputname='Kout';
delaysys.outputname='delaytau';

mdyn=tf(1,[tc 1]);
mdyn.inputname='delaytau';
mdyn.outputname='tauh';


if strcmp(flag,'output')

sys0=connect(Plant,Ksys,delaysys,mdyn,'taur',{'y1','y3'});
elseif strcmp(flag,'input')
    sys0=connect(Plant,Ksys,delaysys,mdyn,'taur',{'tauh'});
elseif strcmp(flag,'delta')
    subblock=sumblk('dy','y3','y1','+-');
    sys0=connect(subblock,Plant,Ksys,delaysys,mdyn,'taur',{'dy'});
else
    error('Not a recognized system formulation')
end

dsys0=c2d(sys0,T);
```

Appendix B

System matrices for G using $\hat{\theta}_0$:

$$A = \begin{bmatrix} 1.01 & 0.115 & 0.138 & 0.077 & -0.000385 & 8.57e-05 & -0.000487 & 9.3e-05 & -0.000844 & -0.00371 \\ 0.845 & 1.82 & 6.47 & 2.67 & -0.00616 & -0.000207 & -0.00784 & -0.000225 & -0.0137 & -0.0478 \\ -0.005 & -0.0106 & 0.972 & 0.0527 & 0.000249 & -5.66e-05 & 0.000314 & -6.14e-05 & 0.000545 & 0.00241 \\ -0.565 & -0.543 & -2.94 & -0.658 & 0.00407 & 7.64e-05 & 0.00517 & 8.33e-05 & 0.00905 & 0.032 \\ -6.92e-05 & -5.31e-05 & -0.00042 & -0.000117 & -3.02e-07 & 2.3e-08 & -3.89e-07 & 1.88e-08 & -6.9e-07 & -2.59e-06 \\ -0.00646 & -0.00465 & -0.0232 & -0.0101 & 8.92e-06 & 4.43e-06 & 1.13e-05 & 4.82e-06 & 1.97e-05 & 3.88e-05 \\ 0.242 & 0.184 & 1.38 & 0.408 & 0.000882 & -6.29e-05 & 0.00112 & -6.82e-05 & 0.00195 & 0.00752 \\ 4.13 & 3.02 & 14.5 & 6.52 & -0.00909 & -0.00312 & -0.0115 & -0.00338 & -0.02 & -0.0497 \\ -41.7 & -31.4 & -267 & -74 & -0.152 & 0.016 & -0.193 & 0.0174 & -0.336 & -1.33 \\ -30.7 & -22.9 & -165 & -52.6 & 0.0103 & 0.0218 & 0.0131 & 0.0236 & 0.0227 & -0.0775 \end{bmatrix}$$

$$B = \begin{bmatrix} 0.00157 \\ 0.0297 \\ -0.000627 \\ -0.0117 \\ -1.47e-07 \\ 9.31e-06 \\ 0.000416 \\ -0.00138 \\ -0.0458 \\ -0.0147 \end{bmatrix}$$

$$C = \begin{bmatrix} 1 & 0 & 0 & 0 & 0 & 0 & 0 & 0 & 0 & 0 \\ 0 & 0 & 1 & 0 & 0 & 0 & 0 & 0 & 0 & 0 \end{bmatrix}$$

System matrices for G_δ using $\hat{\theta}_0$:

$$A = \begin{bmatrix} 1.01 & 0.115 & 0.138 & 0.077 & -0.000385 & 8.57e-05 & -0.000487 & 9.3e-05 & -0.000844 & -0.00371 \\ 0.845 & 1.82 & 6.47 & 2.67 & -0.00616 & -0.000207 & -0.00784 & -0.000225 & -0.0137 & -0.0478 \\ -0.005 & -0.0106 & 0.972 & 0.0527 & 0.000249 & -5.66e-05 & 0.000314 & -6.14e-05 & 0.000545 & 0.00241 \\ -0.565 & -0.543 & -2.94 & -0.658 & 0.00407 & 7.64e-05 & 0.00517 & 8.33e-05 & 0.00905 & 0.032 \\ -6.92e-05 & -5.31e-05 & -0.00042 & -0.000117 & -3.02e-07 & 2.3e-08 & -3.89e-07 & 1.88e-08 & -6.9e-07 & -2.59e-06 \\ -0.00646 & -0.00465 & -0.0232 & -0.0101 & 8.92e-06 & 4.43e-06 & 1.13e-05 & 4.82e-06 & 1.97e-05 & 3.88e-05 \\ 0.242 & 0.184 & 1.38 & 0.408 & 0.000882 & -6.29e-05 & 0.00112 & -6.82e-05 & 0.00195 & 0.00752 \\ 4.13 & 3.02 & 14.5 & 6.52 & -0.00909 & -0.00312 & -0.0115 & -0.00338 & -0.02 & -0.0497 \\ -41.7 & -31.4 & -267 & -74 & -0.152 & 0.016 & -0.193 & 0.0174 & -0.336 & -1.33 \\ -30.7 & -22.9 & -165 & -52.6 & 0.0103 & 0.0218 & 0.0131 & 0.0236 & 0.0227 & -0.0775 \end{bmatrix}$$

$$B = \begin{bmatrix} 0.00157 \\ 0.0297 \\ -0.000627 \\ -0.0117 \\ -1.47e-07 \\ 9.31e-06 \\ 0.000416 \\ -0.00138 \\ -0.0458 \\ -0.0147 \end{bmatrix}$$

$$C = \begin{bmatrix} -1 & 0 & 1 & 0 & 0 & 0 & 0 & 0 & 0 & 0 \end{bmatrix}$$

System matrices for G_u using $\hat{\theta}_0$:

$$A = \begin{bmatrix} 1.01 & 0.115 & 0.138 & 0.077 & -0.000385 & 8.57e-05 & -0.000487 & 9.3e-05 & -0.000844 & -0.00371 \\ 0.845 & 1.82 & 6.47 & 2.67 & -0.00616 & -0.000207 & -0.00784 & -0.000225 & -0.0137 & -0.0478 \\ -0.005 & -0.0106 & 0.972 & 0.0527 & 0.000249 & -5.66e-05 & 0.000314 & -6.14e-05 & 0.000545 & 0.00241 \\ -0.565 & -0.543 & -2.94 & -0.658 & 0.00407 & 7.64e-05 & 0.00517 & 8.33e-05 & 0.00905 & 0.032 \\ -6.92e-05 & -5.31e-05 & -0.00042 & -0.000117 & -3.02e-07 & 2.3e-08 & -3.89e-07 & 1.88e-08 & -6.9e-07 & -2.59e-06 \\ -0.00646 & -0.00465 & -0.0232 & -0.0101 & 8.92e-06 & 4.43e-06 & 1.13e-05 & 4.82e-06 & 1.97e-05 & 3.88e-05 \\ 0.242 & 0.184 & 1.38 & 0.408 & 0.000882 & -6.29e-05 & 0.00112 & -6.82e-05 & 0.00195 & 0.00752 \\ 4.13 & 3.02 & 14.5 & 6.52 & -0.00909 & -0.00312 & -0.0115 & -0.00338 & -0.02 & -0.0497 \\ -41.7 & -31.4 & -267 & -74 & -0.152 & 0.016 & -0.193 & 0.0174 & -0.336 & -1.33 \\ -30.7 & -22.9 & -165 & -52.6 & 0.0103 & 0.0218 & 0.0131 & 0.0236 & 0.0227 & -0.0775 \end{bmatrix}$$

$$B = \begin{bmatrix} 0.00157 \\ 0.0297 \\ -0.000627 \\ -0.0117 \\ -1.47e-07 \\ 9.31e-06 \\ 0.000416 \\ -0.00138 \\ -0.0458 \\ -0.0147 \end{bmatrix}$$

$$C = \begin{bmatrix} 0 & 0 & 0 & 0 & 0 & 0 & 0 & 0 & 0 & 2.53 \end{bmatrix}$$